Annals of Biomedical Engineering
https://doi.org/10.1007/s10439-024-03587-w

BMES BIOMEDICAL ENGINEERING SOCIETY

ORIGINAL ARTICLE

Analysis of Energy and Pressure in the Sinus with Different Blood Pressures after Bioprosthetic Aortic Valve Replacement

Brennan Vogl[1] · Agata Sularz[2] · Sunyoung Ahn[1] · Rajat Gadhave[1] · Scott Lilly[3] · Vinod Thourani[4] · Brian Lindman[5] · Mohamad Alkhouli[2] · Hoda Hatoum[1,6]

Received: 19 April 2024 / Accepted: 11 July 2024

Abstract

Purpose To investigate the effect of changing systolic and diastolic blood pressures (SBP and DBP, respectively) on sinus flow and valvular and epicardial coronary flow dynamics after TAVR and SAVR.

Methods SAPIEN 3 and Magna valves were deployed in an idealized aortic root model as part of a pulse duplicating left heart flow loop simulator. Different combinations of SBP and DBP were applied to the test setup and the resulting change in total coronary flow from baseline (120/60 mmHg), effective orifice area (EOA), and left ventricular (LV) workload, with each combination, was assessed. In addition, particle image velocimetry was used to assess the Laplacian of pressure ($\nabla^2 P$) in the sinus, coronary and main flow velocities, the energy dissipation rate (EDR) in the sinus and the LV workload.

Results This study shows that under an elevated SBP, there is an increase in the total coronary flow, EOA, LV workload, peak velocities downstream of the valve, $\nabla^2 P$, and EDR. With an elevated DBP, there was an increase in the total coronary flow and $\nabla^2 P$. However, EOA and LV workload decreased with an increase in DBP, and EDR increased with a decrease in DBP.

Conclusions Blood pressure alters the hemodynamics in the sinus and downstream flow following aortic valve replacement, potentially influencing outcomes in some patients.

Keywords Hypertension · Particle image velocimetry · Coronary flow · Transcatheter aortic valve replacement · Surgical aortic valve replacement

Associate Editor Stefan M. Duma oversaw the review of this article.

✉ Hoda Hatoum
hhatoum@mtu.edu

[1] Department of Biomedical Engineering, Michigan Technological University, 1400 Townsend Dr, Houghton, MI 49931, USA

[2] Department of Cardiovascular Medicine, Mayo Clinic, Rochester, MN, USA

[3] Department of Cardiovascular Medicine, The Ohio State University, Columbus, OH, USA

[4] Department of Cardiovascular Surgery, Piedmont Heart Institute, Marcus Valve Center, Atlanta, GA, USA

[5] Division of Cardiovascular Medicine, Structural Heart and Valve Center, Vanderbilt University Medical Center, Nashville, TN, USA

[6] Health Research Institute, Center of Biocomputing and Digital Health and Institute of Computing and Cybersystems, Michigan Technological University, Houghton, MI, USA

Abbreviations

AVR	Aortic valve replacement
SAVR	Surgical aortic valve replacement
TAVR	Transcatheter aortic valve replacement
SBP	Systolic blood pressure
DBP	Diastolic blood pressure
SAV	Surgical aortic valve
TAV	Transcatheter aortic valve
EOA	Effective orifice area
PIV	Particle image velocimetry
EDR	Energy dissipation rate
VHD	Valve hemodynamic deterioration
HALT	Hypoattenuating leaflet thickening

Introduction

Aortic stenosis is one of the most common forms of aortic valve disease and it necessitates aortic valve replacement in most of the cases [1]. Surgical and transcatheter aortic valve replacement (SAVR and TAVR, respectively) are the

Published online: 05 August 2024

recommended treatments for clinically significant aortic stenosis.

Immediately after SAVR and TAVR, patients often experience changes in blood pressure that may be clinically consequential [2]. Lindman et al. have shown that patients with elevated blood pressures after TAVR and SAVR had better outcomes and improved survival rates [3]. In contrast, lower blood pressures after valve replacement (< 120/60 mmHg) were associated with increased all-cause and cardiovascular mortality [3]. There is currently no specific guidance for blood pressure regulation after aortic valve replacement. These observations prompt efforts to understand how alterations in blood pressure after valve replacement may be related to clinical outcomes.

Studies have quantified and documented changes in sinus and coronary flow dynamics after aortic valve replacement (AVR) [4–10], but not with varying blood pressures. Additionally, controlled systematic studies to better understand the ventriculo-aortic-arterial interactions in the setting of AVR and different blood pressures, are limited. The addition of these studies may shed light on the interrelationships between these observations and provide a characterization of what the hemodynamic environment undergoes under these conditions. We have previously investigated flow dynamics in the sinus and downstream of the valve after AVR at different blood pressure conditions [11–13]. However, a complete understanding of the blood pressure effect on sinus and epicardial coronary flow dynamics after AVR has not been performed.

In this study, we aim to investigate the effect of changing systolic and diastolic blood pressures (SBP and DBP, respectively) on sinus flow, valvular and epicardial coronary flow dynamics and energetics after TAVR and SAVR.

Methods

Hemodynamic Assessment

A 25 mm Magna surgical aortic valve (SAV) and an uncrimped 26 mm SAPIEN 3 transcatheter aortic valve (TAV), were deployed in an aortic root chamber of a pulse duplicating left heart flow loop simulator [10, 13, 14]. The simulator (Fig. 1) consisted of a fluid reservoir for the blood analog (water-glycerin, 60–40% in volume), a mechanical mitral valve separating the fluid reservoir and pump, a pump controlled by an in-house LabVIEW (National Instruments, TX, USA) program, a rigid idealized aortic root model, a compliance chamber to simulate arterial distensibility, a gate valve to control the aortic flow, a pinch valve to control the total coronary flow, and ultrasound clamp-on flow rate sensors (Transonic, NY, USA) to measure the flows before the valve and in the total coronary branch. Details on the aortic root chamber can be found in a previous publication [15] and in Supplementary Figure 1. Out of the aortic chamber sinus,

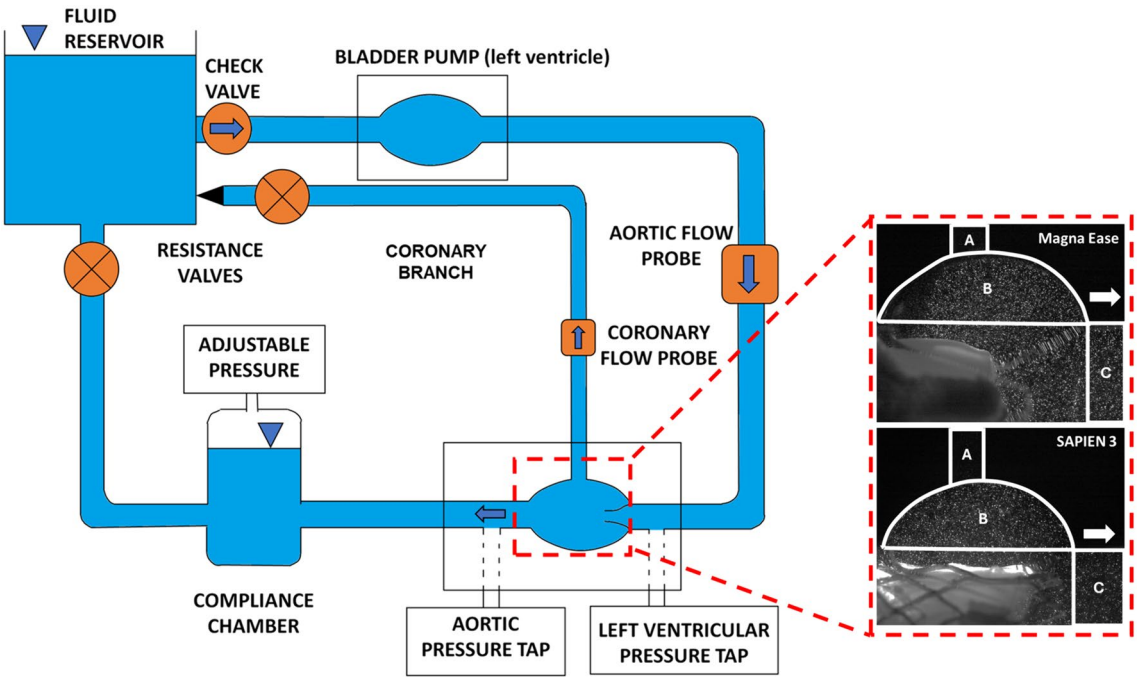

Fig. 1 Schematic diagram showing the left heart simulator experimental setup and the regions of interest for both valves. A = coronary; B = sinus; C = downstream of the valve. The arrows indicate the direction of flow.

we extended a connection that represented the total coronary branch. The cardiac output was 5 L/min, and a heart rate of 60 bpm was used. The total coronary flow was calculated to be 4–5% of the cardiac output resulting in an average total coronary flow range between 200 and 250 mL/min. The average coronary flow was calibrated within these physiological limits at 120/60 mmHg by controlling the resistance of the total coronary circuit at the start of the experiment. After the baseline physiological coronary condition was achieved, the total coronary flow was left to vary as the SBPs (100, 120, 160 mmHg) and DBPs (40, 60, 90 mmHg) were changed. This procedure was chosen so that only the effect of the different blood pressure combinations on the total coronary flow were assessed. The aortic and ventricular pressures were measured throughout each cardiac cycle with Millar catheters (ADinstruments, CO, USA). A total of fifty consecutive cardiac cycles of pressure and flow rate data were recorded at a sampling rate of 100 Hz. Ensemble averaged waveforms of aortic pressure for all the blood pressure conditions are shown in Supplementary Figure 2.

The effective orifice area (EOA) was computed using Gorlin's equation [16] as follows:

$$EOA = \frac{Q_{rms}\left(\frac{\mathrm{cm}^3}{s}\right)}{51.6\sqrt{\Delta P(\mathrm{mmHg})}}. \tag{1}$$

Where Q_{rms} is the root mean square value of the flow rate and ΔP is the average transvalvular pressure gradient defined as the average of the positive pressure difference between the ventricular and aortic pressure curves during forward flow. The Gorlin equation is used to evaluate valve performance by relating valve area to blood flow and pressure. The effective orifice area is the net area of the vena contracta and is a well-established measure of prosthetic heart valve efficiency [17]. A higher EOA is considered better because a larger area is available for the fluid to pass through.

The left ventricular workload was calculated for each case based on the following equation:

$$W = \int_0^T P(t)\mathrm{d}V(t). \tag{2}$$

Where $P(t)$ and $V(t)$ are the instantaneous pressure and volume, respectively, and T is the length of time for a single cardiac cycle.

Particle Image Velocimetry (PIV)

PIV was used to extract the flow properties downstream of the valve and at the entrance of the total coronary branch for each blood pressure condition. Rhodamine B particles with an average size of 10 µm were seeded into the blood analog, the aforementioned regions of interest were illuminated using a laser sheet created by a pulsed Nd:YLF single cavity diode pumped solid state laser coupled with external spherical and cylindrical lenses while acquiring high-speed images of the fluoresced particles' displacement and movement. Time-resolved PIV images were acquired at a temporal resolution of 4000 Hz. Refraction was corrected using a calibration in DaVis PIV software (DaVis 10, LaVision Germany). Velocity vectors were calculated in DaVis using advanced PIV cross-correlation approaches with a 50% overlap multi-pass approach starting from one 32×32-pixel interrogation followed by two 16×16-pixel interrogation passes. Post processing was performed using adaptive median filtering. This was performed like that of other published works by our group [4–8, 18–20].

The Laplacian of the pressure ($\nabla^2 P$) through the Poisson equation for pressure was computed as follows:

$$\frac{-1}{\rho}\left(\frac{\partial^2 P}{\partial x^2} + \frac{\partial^2 P}{\partial y^2}\right) = \left(\frac{\partial V_x}{\partial x}\right)^2 + 2\frac{dV_x}{dy}\frac{\partial V_y}{\partial x} + \left(\frac{\partial V_y}{\partial y}\right)^2. \tag{3}$$

Where ρ is the density in Kg/m^3, P the pressure in Pa, V_x and V_y are the x and y components of the velocity vector in m/s. The x and y directions are axial and lateral respectively. The Laplacian of the pressure is the divergence of the gradient of the pressure field, and its physical significance is in its ability to help identify the changes in the pressure field [21]. Through $\nabla^2 P$, the difference of the field value from the surrounding regions of the sinus can be assessed.

The energy dissipation rate (EDR) per unit volume in the sinus was computed using the method described by Okafor et al. and Hatoum et al. [22, 23]. The equation used is as follows:

$$EDR = \mu\left[\left(\frac{\partial V_x}{\partial x}\right)^2 + \left(\frac{\partial V_y}{\partial y}\right)^2 + 0.5\left(\left(\frac{\partial V_x}{\partial y}\right) + \left(\frac{\partial V_y}{\partial x}\right)\right)^2\right] \tag{4}$$

Where µ is the viscosity with a value of 3.5cP, and V_x and V_y are the x and y components of the velocity vector in m/s.

Results

Coronary Flow

The total coronary flow waveforms for each valve and blood pressure combination are shown in Figure 2. In all cases, elevated SBP and DBP resulted in a higher total coronary flow. As SBP increased from 100 to 160 mmHg, the total coronary flow for the SAPIEN increased from 203.87 ± 29.75 to 255.9 ± 63.14 mL/min ($p < 0.0001$) and the Magna increased from 201.73 ± 63.13 to 287.32 ± 68.16 mL/min ($p < 0.0001$). As DBP increased from 40 to 90 mmHg, the total coronary

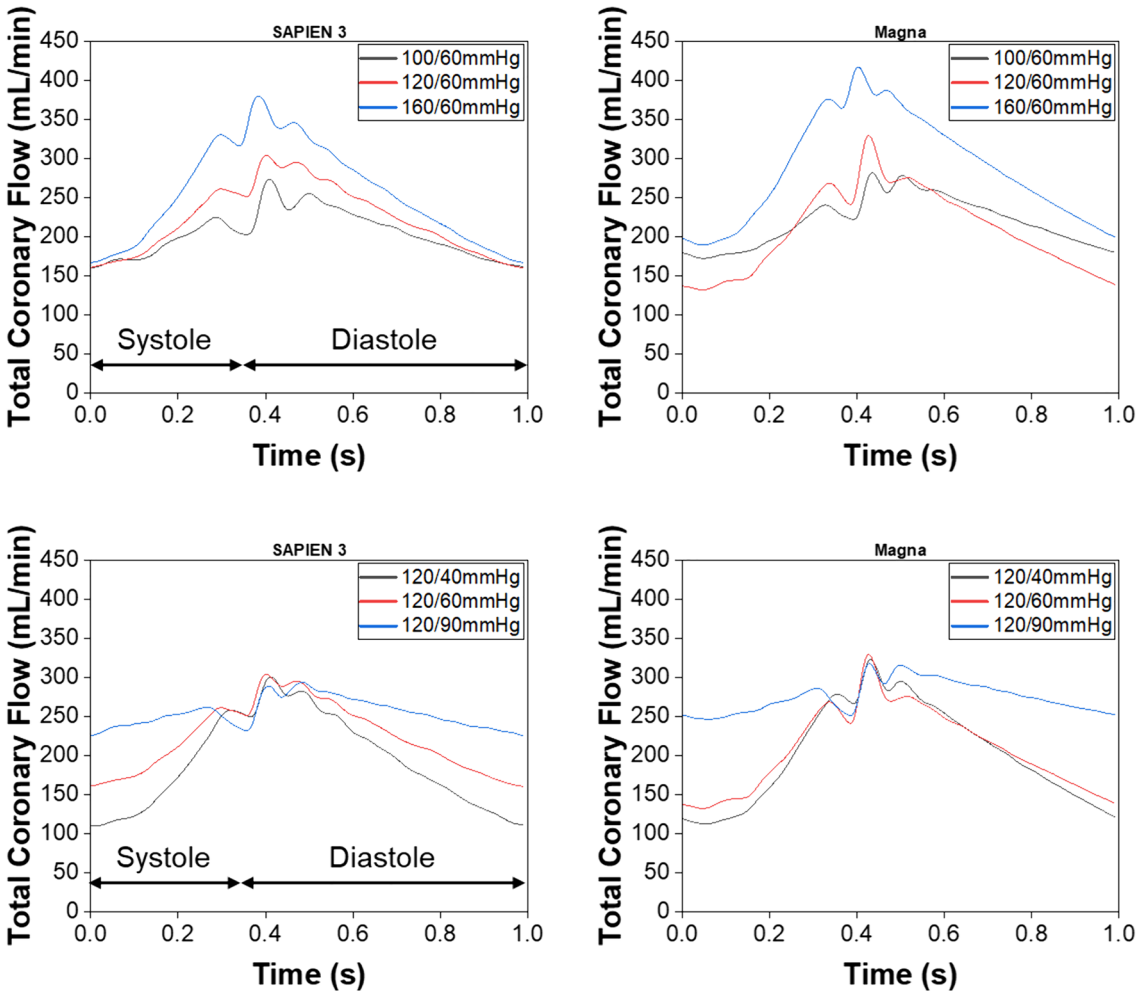

Fig. 2 Ensemble averaged coronary flow variations versus time for the SAPIEN 3 and the Magna under different combinations of SBP (top) and DBP (bottom).

flow for the SAPIEN increased from 192.33 ± 59.07 to 254.24 ± 18.74 mL/min ($p < 0.0001$) and the Magna increased from 201.73 ± 63.13 to 275.18 ± 20.15 mL/min ($p < 0.0001$). The waveforms' slope at the rise and decay segments were different depending on the pressure. With both valves, as SBP increased from 100 to 160 mmHg, a higher systolic slope and a higher diastolic peak was observed. In addition, as DBP increased from 40 to 90 mmHg, the rising systolic slope decreased, and the diastolic peaks were comparable for each pressure.

Hemodynamic Parameters

The EOA of each valve at each blood pressure combination is shown in Figure 3. The variation in EOA did not exceed 0.35 cm^2 between blood pressure conditions. As SBP increased from 100 to 160 mmHg, the SAPIEN 3 EOA increased from 1.88 ± 0.03 to 1.98 ± 0.02 cm^2 ($p < 0.0001$) and the Magna increased from 2.35 ± 0.03 to 2.56 ± 0.04 cm^2 ($p < 0.0001$).

As DBP increased from 40 to 90 mmHg, the SAPIEN 3 EOA decreased from 1.91 ± 0.03 to 1.90 ± 0.04 cm^2 ($p = 1.0$) and the Magna decreased from 2.61 ± 0.03 to 2.26 ± 0.03 cm^2 ($p < 0.0001$) with the Magna.

Velocity Downstream of the Valve and at the Intersection of the Coronary Ostium and the Sinus

The variation of velocity downstream of the valve versus time is shown in Fig. 4 (measurement was taken at 1.5 mm from the STJ limit for both valves). While the changes in velocity magnitudes were not significant between the different cases when SBP increased, the higher the SBP the higher the fluctuations were found. Velocities specifically during acceleration were lower with an increase in SBP for both

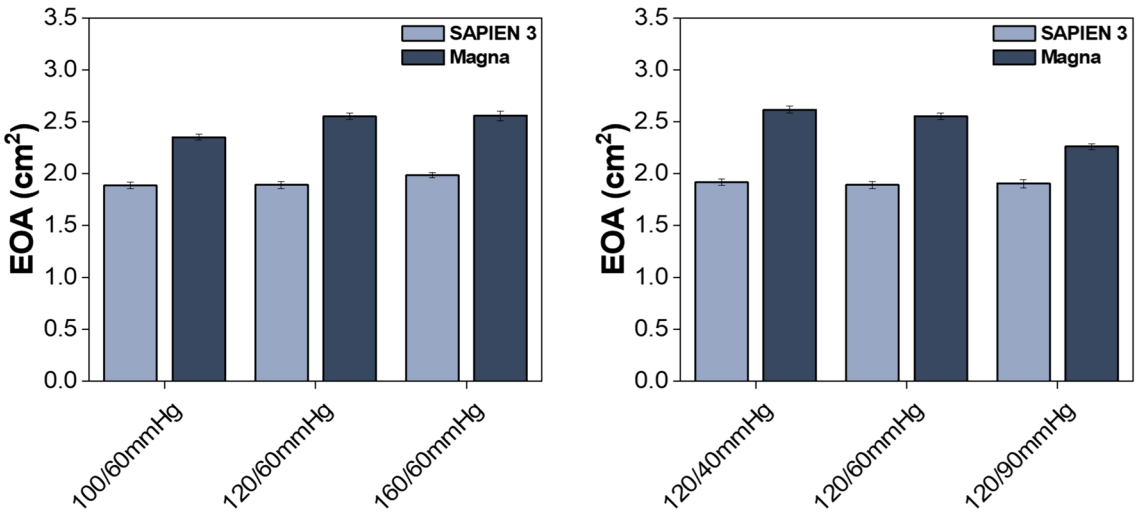

Fig. 3 Average EOA for the SAPIEN 3 and Magna valves for each of the different blood pressure conditions. The error bars represent the standard deviations.

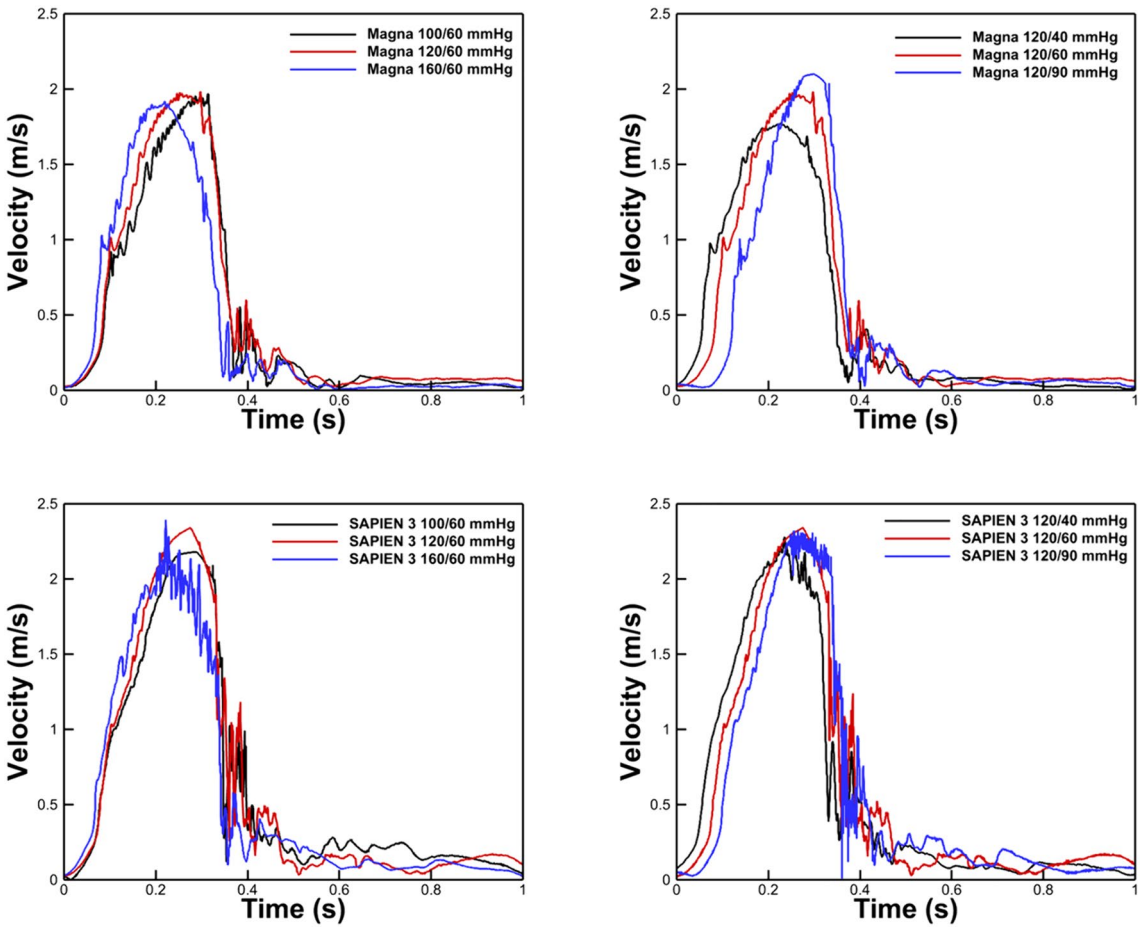

Fig. 4 Variations of the instantaneous velocity downstream of the SAPIEN 3 and Magna under different combinations of SBP (top) and DBP (bottom).

valves, however the peak was higher. The increase in DBP led to an increase in peak velocity, however, during acceleration, the higher DBP was associated with lower velocities. Fluctuations during deceleration were more obvious with the SAPIEN 3.

The variation of velocity at the coronary entrance is shown in Figs 5 and 6. The flow velocity at the coronary entrance shows larger fluctuations at the highest SBP and DBP.

Laplacian of Pressure ($\nabla^2 P$) in the Sinus

With changing aortic blood pressure, it is important to assess the changes in the sinus pressure. Contour plots for the Laplacian of pressure for both valves and the different pressure combinations are shown in Figs 7 and 8.

As SBP increased from 100 to 160 mmHg, both valves had an area increase of the $\nabla^2 P$. A similar trend was observed when increasing DBP from 40 to 90 mmHg. The coronary entrance was one of the main regions in the sinus where $\nabla^2 P$ was most pronounced and more negative than the surrounding regions.

Energy Dissipation Rate

EDR results for both valves and each pressure combination are shown in Fig. 9. An increase in SBP generally resulted in an increase in EDR. However, an increase in DBP was associated with a decrease in EDR.

Left Ventricular Workload

LV workload for each blood pressure combination and valve is shown in Fig. 10. An increase in workload was observed for both valves with an increase in SBP. As SBP increased from 100 to 160 mmHg, the SAPIEN 3 LV workload increased from 0.37 ± 0.01 to 0.95 ± 0.02 J ($p < 0.0001$) and the Magna increased from 0.42 ± 0.02 to 0.947 ± 0.03 J ($p < 0.0001$).

An increase in DBP had the opposite effect on workload. As DBP increased from 40 to 90 mmHg, the SAPIEN 3 LV workload decreased from 0.73 ± 0.02 to 0.32 ± 0.01 J ($p < 0.0001$) and the Magna decreased from 0.69 ± 0.02 to 0.51 ± 0.01 J ($p < 0.0001$).

Discussion

This study aimed to provide a detailed assessment of the effect of changing SBP and DBP on valve and coronary hemodynamics after AVR with a TAV SAPIEN 3 and a SAV Magna. It is important to understand how SBP and DBP affect valvular energetics and the resulting epicardial coronary flow in relation to alterations of the pressure.

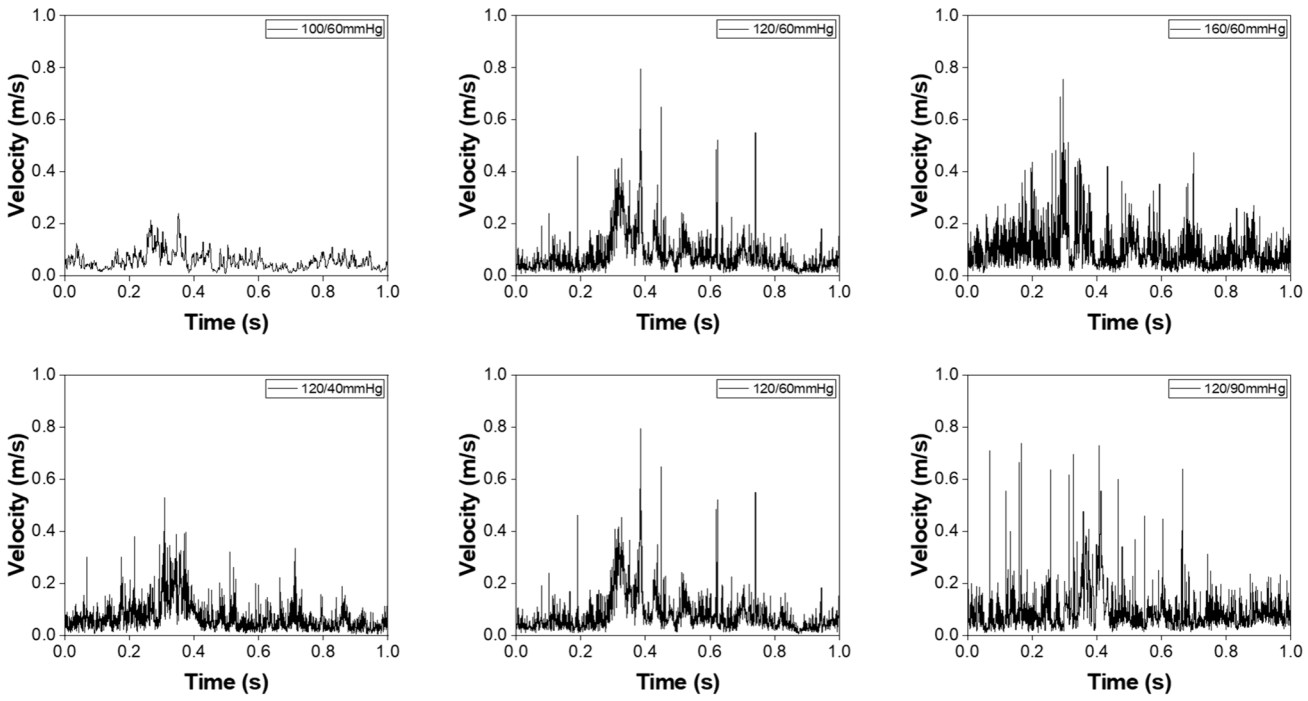

Fig. 5 Variations of the instantaneous velocity at the total coronary entrance for the SAPIEN 3 under different combinations of SBP (top) and DBP (bottom).

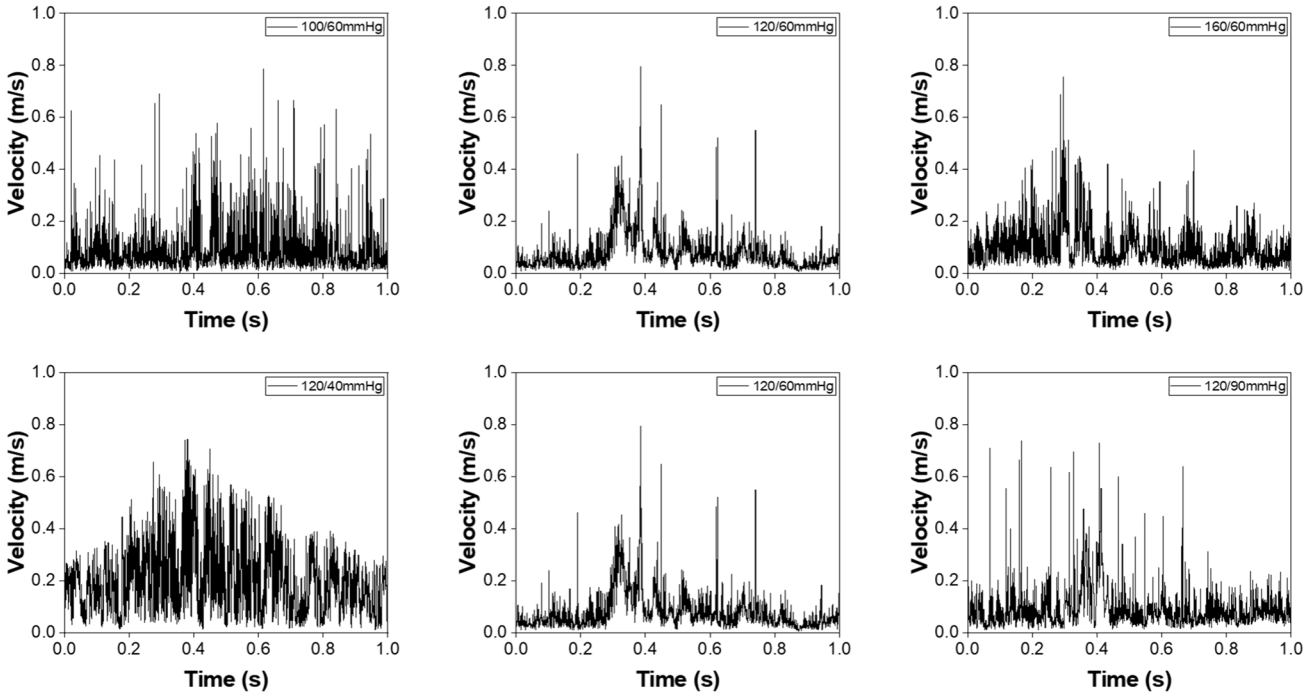

Fig. 6 Variations of the instantaneous velocity at the total coronary entrance for the Magna under different combinations of SBP (top) and DBP (bottom).

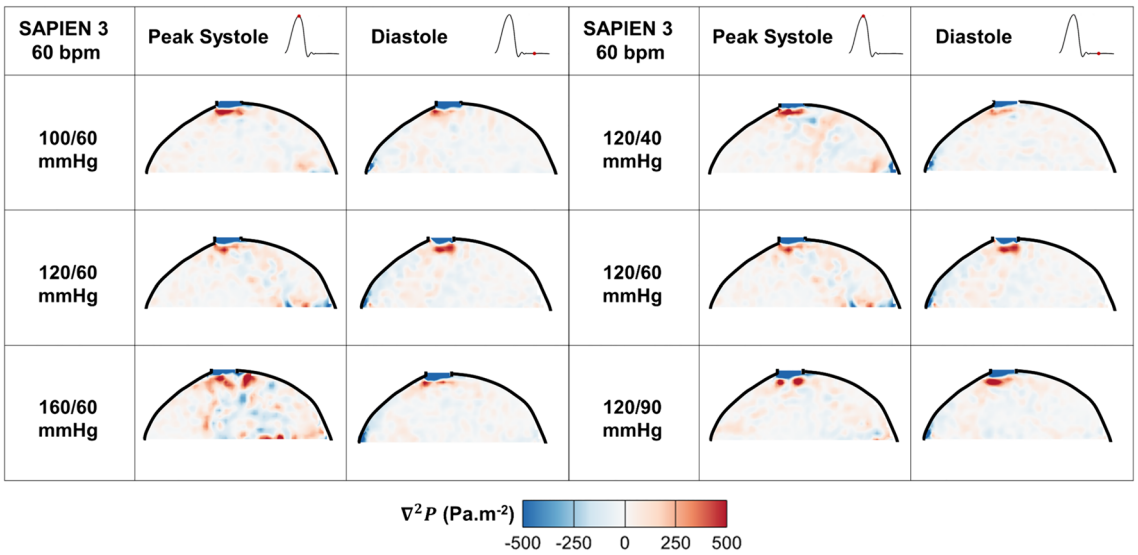

Fig. 7 Laplacian of pressure contours in the sinus and the coronary entrance in the presence of a SAPIEN 3.

The results obtained in this study showed that the rise and decay of the coronary flow waveforms were different as DBP changed. A decrease in DBP led to sharper rise and decay of the coronary flow waveform, with significantly lower mean flow. These results can be explained through the role of DBP in coronary perfusion. Generally, physiologically low DBP has been associated with myocardial ischemia [24, 25] and is a key factor in coronary perfusion pressure (CPP; Equation 5).

$$CPP = DBP - LVEDP \tag{5}$$

Where *LVEDP* is the left ventricular end diastolic pressure. At the coronary entrance in all the cases, a more negative $\nabla^2 P$ was observed at the ostium indicating a lower

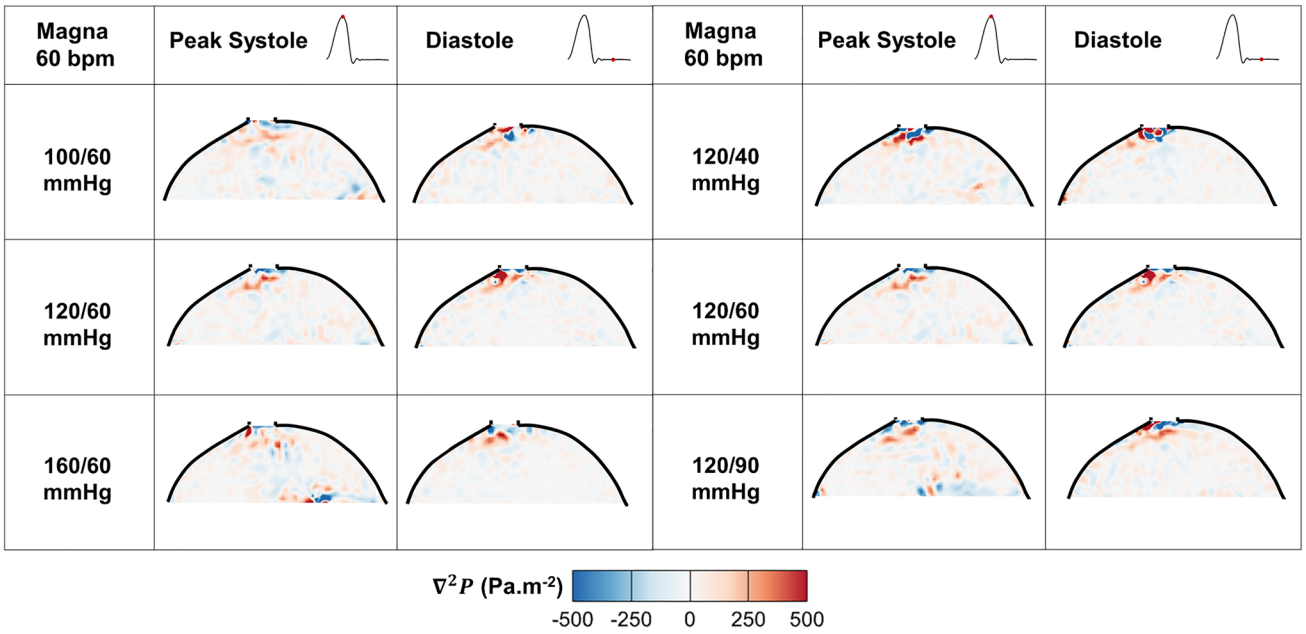

Fig. 8 Laplacian of pressure contours in the sinus and the coronary entrance in the presence of a Magna.

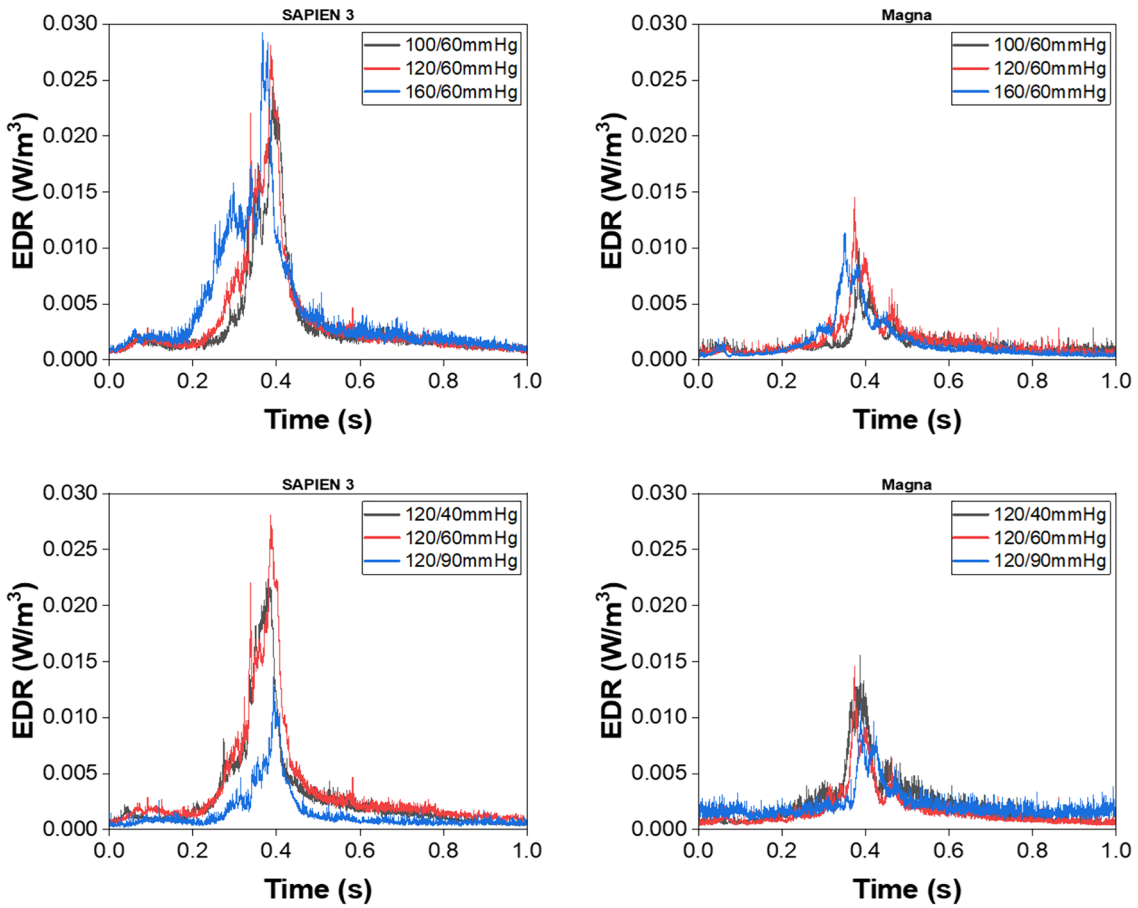

Fig. 9 Energy dissipation rate (EDR) for the SAPIEN 3 and Magna in the sinus under different SBP (top) and DBP (bottom) conditions.

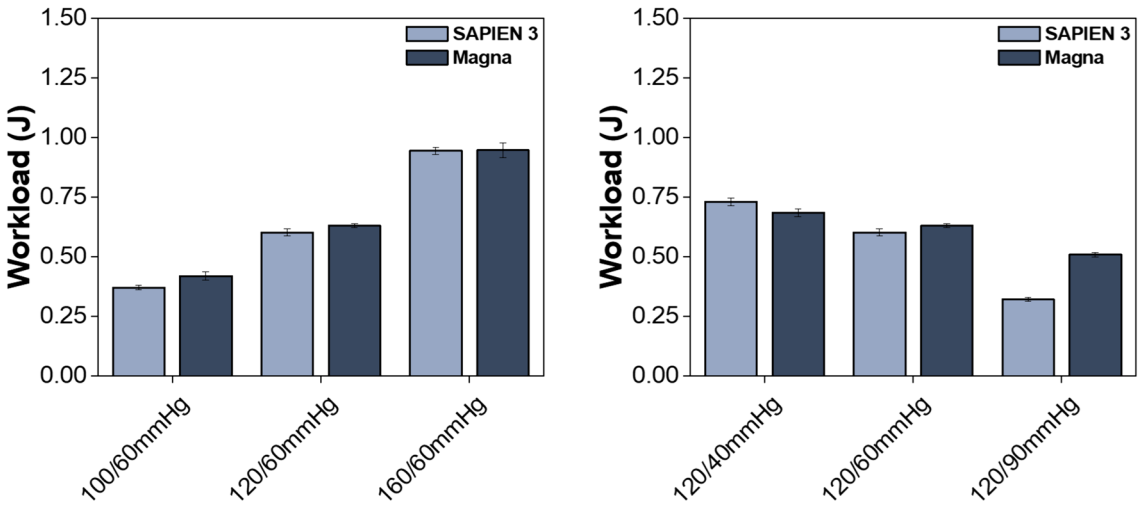

Fig. 10 Average left ventricular workload for the SAPIEN 3 and Magna valves for each of the different blood pressure conditions. The error bars represent the standard deviations.

pressure in this region compared with the surroundings as SBP and DBP increased. As previously mentioned, evaluating $\nabla^2 P$ in the sinus provides information on how different the field value (pressure) is with respect to the surrounding. Therefore, from the results, it seems that as SBP and DBP increase, the flow is encouraged (sink effect) to enter the coronary due to the much lower pressure at the entrance. These results are the same as what was conjectured by Lindman et al. [3]

An increase in SBP led to a significant upward shift in the coronary flow curve, with a clear increase in mean coronary flow. Additionally, the rise and decay of the waveforms were almost parallel. Within the aortic pressure waveform, SBP occurs due to the stretch that large arteries undergo to accommodate the systolic ejection volume. As SBP increases, the metabolic demands of the myocardium increase, leading to a potential increase in the coronary flow [26].

The results of this study showed that SBP and DBP had a minor effect on EOA from a clinical standpoint. In a clinical study by Kadem et al. [27], it was shown that an increase in SBP may result in an increase of the leaflets opening and thus the EOA. The DBP may not provide a significant change in EOA given that the valve is closed and the pressure in the heart is at rest rather than a state of active pumping.

The velocity results showed that as DBP increased from 40 to 90 mmHg, the velocity downstream of the aortic valve was higher during systole. Although this velocity is downstream from the valve, the modified Bernoulli equation, if applied, would yield elevated transvalvular pressure gradients with higher velocities and therefore lower EOAs. This being said, the results showed that peak velocities were not very different at 160/60 mmHg compared to 100/60 mmHg, and the EOA was higher with the 160/60 mmHg case. This result is consistent with what would be expected despite the more apparent vigorous fluctuations in velocity at the more elevated blood pressures.

Energy dissipation is the result of fluid instabilities, mixing, in addition to transfer of momentum and kinetic energy to the smaller scales in the flow where it is ultimately converted to heat through viscosity [22]. This study showed that with an increasing SBP, energy dissipation increases. In a previous study by our team [11], we demonstrated that an increase in SBP leads to significant increase in velocity, vorticity, and vorticity fluctuations within the sinus. This can lead to increased mixing and instabilities, resulting in elevated energy dissipation [22, 28]. The SAPIEN 3 was characterized with more elevated energy dissipation, likely due to the inherent valve design differences (presence of the stent) in addition to a smaller EOA [9, 15]. We then found in this study that a decrease in DBP led to an increase in energy dissipation. A decreasing DBP is associated with an elevated workload [29] and energy consumption, leading to inefficient energy use and increased dissipation.

Another way to interpret these results would be to consider the change in pulse pressure (difference between systolic and diastolic blood pressures). A wider pulse pressure led to an increase in energy dissipation and LV workload. Generally, a wide pulse pressure is an indicator of vascular stiffening and reduction in compliance, in addition to a sign that the ventricle is working harder to pump blood into the aorta [30]. This typically leads to a compromised ability to store and gradually release energy, which leads to more dissipation and increased LV workload.

Clinical Implications of High vs. low SBP and High vs. Low DBP

Our study documented the mechanical changes on the flow in the sinus, downstream the aortic valve, and within the immediate coronary artery. These changes help in understanding several relationships that are relevant to disease progression such as leaflet thrombosis after valve replacement and myocardial infarctions. Several groups have observed positive outcomes in patients who developed a high SBP following AVR [3, 31–33].

Ischemic stroke rates have been reported to be lower for these patients [34]. In a previous study by our group, we found that the guideline pressure of 120/60 mmHg in a patient with near total occlusion of the right coronary artery, resulted in reduced epicardial coronary flow compared to a hypertensive condition, which may have been the cause of myocardial ischemia[12]. In this study, we showed that elevated SBP and DBP were associated with an overall higher total coronary flow. In addition, the area of negative $\nabla^2 P$ increased with an increase in pressure, especially for an increase in DBP. Again, this result indicates the encouragement of flow from the sinus into the coronary, which translates to a potentially higher total coronary flow. Hypertension may potentially alter energy dissipation and act as an indicator for a patient's health [35]. We found differences in the EDR with changing SBP and DBP, generally wider pulse pressures had a higher EDR. However, it is still unclear whether this indicates a worse outcome for the patient in the long term. Further studies are needed to better understand the relationship between energy dissipation in the aortic root and blood pressure. Outcomes after 1 year for TAVR patients with elevated blood pressures compared to the general population, have been mostly positive [3, 31]. Although, these outcomes are positive [3, 31], it is still unclear how prolonged or chronic hypertension will affect these patients. A potential long-term issue would be the development of hypertrophy due to the increased demand on the LV [36]. In this study, we observed an increase in LV workload with an increase in pulse pressure. The strategy for these patients moving forward may be to find an optimal balance between a blood pressure that sufficiently meets the flow demands of the heart while also minimizing LV workload.

Hypoattenuating leaflet thickening (HALT) has been observed following AVR. It is still unclear whether HALT contributes to valve hemodynamic deterioration (VHD) [37–43], but when VHD occurs in bioprosthetic valves, it has important consequences for valve efficiency. A degenerated valve is less efficient which can be characterized by a higher EDR. We have previously shown that elevated blood pressures may encourage calcification of the bioprosthetic valve via increased velocities, vorticity, and shear stress near the leaflets[11], which can also alter the performance and efficiency of the valve. Studies have also shown that elevated pressures affect the interstitial cells of the valve leaflets, potentially promoting valve disease [44, 45]. Both systolic and diastolic blood pressures were associated with measures of left ventricular hypertrophy [46]. The subsequent higher forces exerted on the valve leaflets can lead to structural fatigue and eventually tearing of the leaflets [47]. More studies are needed to fully understand the relationship between higher aortic pressures and VHD. A valve with reduced leaflet motion can alter the sinus flow dynamics [18, 48] which may lead to changes in the epicardial coronary flow.

Limitations

This study had several limitations. First, the aortic root chamber used is rigid. Nevertheless, in our flow simulator, a compliance chamber is placed downstream of the aortic valve to emulate arterial distensibility. Second, our in-vitro setup is not an appropriate system to represent coronary microcirculation, however, it can accurately represent and allow us to extract epicardial coronary flow waveforms. Third, our aortic root chamber does not have a material representing the native leaflets that would be typically present after TAVR.

Conclusions

In summary, this study assessed the impact of varying systolic and diastolic blood pressures on valvular hemodynamic parameters and the variations of the epicardial coronary flow after aortic valve replacement in the presence of SAPIEN 3 and Magna valves. The study showed that SBP and DBP variations affect the valve's EOA and velocity downstream. In addition, the results showed that SBP and DBP affect the coronary waveforms differently and lead to different patterns of pressure in the coronary sinus and different intensities of fluctuations in velocity at the coronary ostium. More energy dissipation was seen with more elevated pulse pressure. To fully understand the complicated relationship between blood pressure and the flow dynamic environment after aortic valve replacement, we believe that controlled animal studies would give a more comprehensive overview of these interactions by assessing the full preload and afterload parameters.

Supplementary Information The online version contains supplementary material available at https://doi.org/10.1007/s10439-024-03587-w.

Funding This research was funded by the National Science Foundation award number 2301649.

Declarations

Competing Interests The authors do not report any relevant conflict of interest. Dr. Lindman has consulted for and received investigator-initiated research grant funding from Edwards Lifesciences and consulted for AstraZeneca.

References

1. Jang, S. Y., et al. Temporal trends in incidence, prevalence, and death of aortic stenosis in Korea: a nationwide population-based study. *ESC Heart Fail*. 9(5):2851–2861, 2022.
2. Yeoh, J. and P. MacCarthy, The pressure is on: implications of blood pressure after aortic valve replacement. 2019, Am Heart Assoc. p. e014631.
3. Lindman, B.R., et al., Blood pressure and arterial load after transcatheter aortic valve replacement for aortic stenosis. Circulation: Cardiovascular Imaging, 2017. **10**(7): p. e006308.
4. Hatoum, H., and L. P. Dasi. Sinus hemodynamics in representative stenotic native bicuspid and tricuspid aortic valves: an in-vitro study. *Fluids*. 3(3):56, 2018.
5. Hatoum, H., et al. Impact of patient-specific morphologies on sinus flow stasis in transcatheter aortic valve replacement: an in vitro study. *J. Thorac. Cardiovasc. Surg.*. 157(2):540–549, 2019.
6. Hatoum, H., et al. Implantation depth and rotational orientation effect on valve-in-valve hemodynamics and sinus flow. *Ann. thorac. surg.* . 106(1):70–78, 2018.
7. Hatoum, H., et al. Sinus hemodynamics variation with tilted transcatheter aortic valve deployments. *Ann. Biomed. Eng.* . 47:75–84, 2019.
8. Hatoum, H., et al., *Aortic sinus flow stasis likely in valve-in-valve transcatheter aortic valve implantation*.J. thorac. cardiovasc. surg. 2017. **154**(1): p. 32-43. e1.
9. Hatoum, H., et al. An in vitro evaluation of turbulence after transcatheter aortic valve implantation. *J. Thorac. Cardiovasc. Surg.* . 156(5):1837–1848, 2018.
10. Vogl, B. J., et al. Flow dynamics in the sinus and downstream of third and fourth generation balloon expandable transcatheter aortic valves. *J. Mech. Behav. Biomed. Mater.* . 127:105092, 2022.
11. Vogl, B., et al., *Effect of blood pressure levels on sinus hemodynamics in relation to calcification after bioprosthetic aortic valve replacement.* Ann. Biomed. Eng. 2023.
12. Vogl, B. J., et al. differential impact of blood pressure control targets on epicardial coronary flow after transcatheter aortic valve replacement. *Struct. Heart*. 8(1):100230, 2024.
13. Vogl, B. J., et al. Impact of blood pressure on coronary perfusion and valvular hemodynamics after aortic valve replacement. *Catheter. Cardiovasc. Interv.* . 99(4):1214–1224, 2022.
14. Zakko, J., et al. Development of tissue engineered heart valves for percutaneous transcatheter delivery in a fetal ovine model. *Basic to Transl. Sci.* . 5(8):815–828, 2020.
15. Vogl, B., et al. Effect of aortic curvature on bioprosthetic aortic valve performance. *J. Biomech.* . 146:111422, 2023.
16. Gorlin, R., and S. G. Gorlin. Hydraulic formula for calculation of the area of the stenotic mitral valve, other cardiac valves, and central circulatory shunts. *Am. Heart J.* . 41(1):1–29, 1951.
17. Yoganathan, A.P., Z. He, and S. Casey Jones, *Fluid mechanics of heart valves.* Annu. Rev. Biomed. Eng., 2004. **6**: p. 331-362.
18. Hatoum, H., and L. P. Dasi. Spatiotemporal complexity of the aortic sinus vortex as a function of leaflet calcification. *Ann. biomed. Eng.* . 47:1116–1128, 2019.
19. Moore, B., and L. P. Dasi. Spatiotemporal complexity of the aortic sinus vortex. *Experiments in Fluids*. 55:1–12, 2014.
20. Hatoum, H., et al. Neosinus and sinus flow after self-expanding and balloon-expandable transcatheter aortic valve replacement. *Cardiovasc. Interv.* . 14(24):2657–2666, 2021.
21. Corral, M., *CORRAL'S VECTOR CALCULUS.*
22. Hatoum, H., B. L. Moore, and L. P. Dasi. On the significance of systolic flow waveform on aortic valve energy loss. *Ann. Biomed. Eng.* . 46:2102–2111, 2018.
23. Okafor, I. U., et al. Role of mitral annulus diastolic geometry on intraventricular filling dynamics. *J. Biomech. Eng.* . 137(12):121007, 2015.
24. Khan, N. A., et al. Effect of lowering diastolic pressure in patients with and without cardiovascular disease: analysis of the SPRINT (Systolic Blood Pressure Intervention Trial). *Hypertension*. 71(5):840–847, 2018.
25. Hsieh, M.-J., et al., *Risk Stratification by Coronary Perfusion Pressure in Left Ventricular Systolic Dysfunction Patients Undergoing Revascularization: A Propensity Score Matching Analysis.* Front. Cardiovasc. Med. 2022. **9**.
26. Rabkin, S. W. Considerations in understanding the coronary blood flow- left ventricular mass relationship in patients with hypertension. *Curr Cardiol Rev*. 13(1):75–83, 2017.
27. Kadem, L., et al. Impact of systemic hypertension on the assessment of aortic stenosis. *Heart*. 91(3):354–361, 2005.
28. Hatoum, H., et al., *The hemodynamics of transcatheter aortic valves in transcatheter aortic valves.* The Journal of thoracic and cardiovascular surgery, 2021. **161**(2): p. 565-576. e2.
29. Tringali, S., and J. Huang. Reduction of diastolic blood pressure: should hypertension guidelines include a lower threshold target? *World J. Hypertens.* . 7(1):1–9, 2017.
30. Tang, K. S., E. D. Medeiros, and A. D. Shah. Wide pulse pressure: a clinical review. *J. Clin. Hypertens.* . 22(11):1960–1967, 2020.
31. Brent, J. K., M. D. Cornelius, and A. H. Thomas. The development or worsening of hypertension after transcatheter aortic valve replacement (TAVR) improves short-term and long-term patient outcomes. *Heart Asia*. 10(2):e010994, 2018.
32. Lindman, B. R., et al. Lower blood pressure after transcatheter or surgical aortic valve replacement is associated with increased mortality. *J. Am. Heart Assoc.* . 8(21):e014020, 2019.
33. Perlman, G.Y., et al., *Post-procedural hypertension following transcatheter aortic valve implantation: incidence and clinical significance.* JACC: Cardiovascular Interventions, 2013. **6**(5): p. 472-478.
34. Koo, H. J., et al. Computed Tomography Features of Cuspal Thrombosis and Subvalvular Tissue Ingrowth after Transcatheter Aortic Valve Implantation. *Am. J. Cardiol.* . 125(4):597–606, 2020.
35. Yap, C.-H., L.P. Dasi, and A.P. Yoganathan, *Dynamic Hemodynamic Energy Loss in Normal and Stenosed Aortic Valves.* J. Biomech. Eng. 2010. **132**(2).
36. Tackling, G. and M.B. Borhade, *Hypertensive heart disease*, in *StatPearls [Internet]*. 2022, StatPearls publishing.
37. Brown, R. A., et al. Subclinical Leaflet Thrombosis Post Transcatheter Aortic Valve Replacement: An Update for 2020. *Struct. Heart*. 4(5):369–381, 2020.
38. Jang, M. H., et al. Impact of leaflet thrombosis on valve haemodynamic status after transcatheter aortic valve replacement. *Heart*. 110(2):140–147, 2024.
39. Rashid, H. N., et al. The impact of hypo-attenuated leaflet thickening on haemodynamic valve deterioration following transcatheter aortic valve replacement. *J. Cardiovasc. Computed Tomography*. 16(2):168–173, 2022.
40. Waksman, R., et al. Transcatheter aortic valve replacement in low-risk patients: 2-year results from the LRT trial. *Am. Heart J.* . 237:25–33, 2021.

41. Hansson, N. C., et al. Transcatheter aortic valve thrombosis: incidence, predisposing factors, and clinical implications. *J. Am. College Cardiol.* . 68(19):2059–2069, 2016.
42. Sellers, S.L., P. Blanke, and J.A. Leipsic, Bioprosthetic heart valve degeneration and dysfunction: focus on mechanisms and multidisciplinary imaging considerations. radiology: cardiothoracic imaging, 2019. **1**(3): p. e190004.
43. Sellers Stephanie, L., et al., Transcatheter aortic heart valves. JACC: cardiovascular imaging, 2019. **12**(1): p. 135-145.
44. Warnock, J. N., et al. Gene Profiling of aortic valve interstitial cells under elevated pressure conditions: modulation of inflammatory gene networks. *Int J Inflam*. 2011:176412, 2011.
45. Xing, Y., et al. Cyclic pressure affects the biological properties of porcine aortic valve leaflets in a magnitude and frequency dependent manner. *Ann. Biomed. Eng.* . 32(11):1461–1470, 2004.
46. Nikorowitsch, J., et al. Correlation of systolic and diastolic blood pressure with echocardiographic phenotypes of cardiac structure and function from three German population-based studies. *Sci. Rep.* . 13(1):14525, 2023.
47. Kupari, M., H. Turto, and J. Lommi. Left ventricular hypertrophy in aortic valve stenosis: preventive or promotive of systolic dysfunction and heart failure? *Eur. heart J.* . 26(17):1790–1796, 2005.
48. Hatoum, H., et al. Predictive model for thrombus formation after transcatheter valve replacement. *Cardiovasc. Eng. technol.* . 12(6):576–588, 2021.